



Copper sulfate reference electrode

Heather A.G. Stern^a, Donald R. Sadoway^{b,*}, Jefferson W. Tester^{a,1}

^a Department of Chemical Engineering, Massachusetts Institute of Technology, Cambridge, MA 02139-4307, United States

^b Department of Materials Science and Engineering, Massachusetts Institute of Technology, Cambridge, MA 02139-4307, United States

ARTICLE INFO

Article history:

Received 28 November 2010

Received in revised form 13 May 2011

Accepted 18 May 2011

Available online 23 June 2011

Keywords:

Copper sulfate electrode

Reference electrode

Liquid junction potential

ELECNRTL

ABSTRACT

The goal of this experimental study was to accurately determine the potential of the copper sulfate electrode (CSE) for use in quantitative electrochemical analysis. The potential of the CSE at 25 °C was found to be 317 mV versus that of the normal hydrogen electrode (NHE), with a slope of 0.17 mV/°C over the range from 5 °C to 45 °C. The determination of the true equilibrium potential of the CSE versus the NHE from laboratory measurements included the estimation of the liquid junction potential (LJP) by means of an electrolyte property model. The value of the LJP was estimated to be –14 mV based on calculated CSE potentials. Direct calculation of the LJP, which should have produced a more accurate result than estimation, failed to do so because the standard assumption of linear concentration variation of all species across the liquid junction was shown to be invalid.

© 2011 Elsevier B.V. All rights reserved.

1. Introduction

The most commonly used aqueous analytical reference electrodes are the saturated calomel electrode (SCE) and the silver–silver chloride (Ag/AgCl) electrode. Not all aqueous systems, particularly those sensitive to chlorides, are best served by these electrodes. An alternative to these is the copper sulfate electrode (CSE) which is composed of a copper wire in contact with an aqueous copper sulfate solution that often contains dilute sulfuric acid. The active electrochemical couple is Cu(s) with Cu²⁺(aq).

The CSE is most commonly used in cathodic or anodic corrosion protection applications of buried metal, such as steel storage tanks and building foundations; hence, it is usually in direct contact with soil. Consequently, the majority of the literature on CSEs is focused on its use in field work, rather than on precise laboratory measurements where accurate electrochemical data are required. The objective of this study was to more accurately determine the potential of the CSE versus the normal hydrogen electrode (NHE) to enable the use of the CSE in analytical studies, including the electrodeposition of copper and other metals. This paper reviews results from previous studies on the CSE and compares them to electrical potential measurements made in the current study. These new data were used as inputs to electrolyte property modeling in order to estimate the liquid junction potential of the system and to determine the true equilibrium potential of the CSE in reference to the NHE.

The general approach outlined in this paper for the CSE could be applied to the development of other reference electrodes. The level of accuracy demanded of any such new reference electrode will dictate whether only the first portion or the entire method presented herein is used. This paper also draws attention to some of the challenges encountered in the development of a new reference electrode.

1.1. Literature review of the copper sulfate electrode

Ewing's [1] work in 1939 laid the foundation for CSE research. His electrode was designed for field use, and there was probably a small amount of sulfuric acid added to the copper sulfate solution. He found that the measured potential difference between a CSE and a SCE with a saturated potassium chloride bridge at 25 °C is "about 75 mV." Ewing also measured the temperature dependence of saturated and unsaturated copper sulfate electrodes over a range from 1 °C to 51 °C versus the potential of an electrode of the same composition held at a constant temperature. The slope of the saturated curve was approximately 0.9 mV/°C. Ewing did not include a correction for the Soret effect of the temperature gradient in the liquid bridge between the two half-cells because the same effect would occur in fieldwork when the soil and half-cell were at different temperatures. Ewing's value for the potential of a CSE has since become one of the standard accepted values [2].

Aker [3] reported on his handmade CSE half-cell for field use. The half-cell contained saturated copper sulfate in water and a porous wooden plug to make the electrical connection. His CSE, versus a SCE, with the half-cells connected by tap water, gave a potential of 70 mV on average, varying from 68 to 73 mV.

* Corresponding author.

E-mail address: dsadoway@mit.edu (D.R. Sadoway).

¹ Present address: Cornell Energy Institute and Atkinson Center for a Sustainable Future, Cornell University, Ithaca, NY 14853, United States.

A more analytical approach to determining the CSE potential (E_{CSE}) was taken by Scott [4]. He claimed that he could extrapolate the activity coefficient of a divalent copper ion up to the saturation point of copper sulfate (1.41 molal at 25 °C) by using data for cadmium and zinc sulfate that spanned that concentration. This claim was based on the fact that copper, cadmium, and zinc sulfate activities coefficients are similar at lower concentrations. The Nernst equation for $\text{Cu} \rightarrow \text{Cu}^{2+} + 2e^-$ at 25 °C (assuming unit activity for solid copper) simplifies to

$$E_{CSE} = E_{CSE}^{\circ} - 0.02958 \log(a_{\text{Cu}^{2+}}) \quad (1)$$

The value for the standard potential of the CSE (E_{CSE}° ; E_{CSE} at 25 °C; activity of Cu^{2+} ($a_{\text{Cu}^{2+}} = 1$) was taken as -0.337 V from Latimer [5], which is close to the value of -0.340 V found in Bard and Faulkner [6]. With $a_{\text{Cu}^{2+}}$ approximated as 0.0390, the calculated value of E_{CSE} is -0.300 V relative to the NHE. A similar calculation yielded a value for E_{CSE} of -0.060 V relative to the SCE. Taking into account the reversed sign convention of Scott [4], the potential would be written today as E_{CSE} equal to $+0.300$ V versus NHE and $+0.060$ V versus SCE. Thus Scott's results are approximately 10–15 mV smaller than the previously published studies.

Scott's study also included an experimental component, in which he studied variation with temperature, along with other properties of the electrodes. He cooled electrodes to 4 °C and allowed them to come to ambient temperature while measuring their potential with respect to a structure in soil. He repeated the experiment with the same set of electrodes first heated to 49 °C. His results had an average slope of 0.97 mV/°C.

More recent studies have focused on factors affecting the accuracy of the CSE. Since copper salts are photosensitive, it was hypothesized that light could be an important factor when using a CSE outdoors. The difference in potential between a CSE in bright sunshine at noon versus a CSE in the dark was found by Ansuini and Dimond [7] to be -52 mV; however, when exposure was from a fluorescent light, the shift was only -2 mV. Ansuini and Dimond also found that a change in copper sulfate concentration resulted in a potential shift of about 20 mV/(decade of g/L). The logarithmic dependence of the potential on concentration is expected, given Eq. (1), since the activity is approximately proportional to the concentration. Ansuini and Dimond also found that chlorides in the electrolyte solution of a CSE have a pronounced effect on the CSE potential. At 1.0% chloride, the CSE potential was shifted negatively by 100 mV.

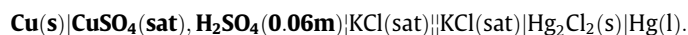
Further work was done by Pawel et al. [8] on the effect of temperature on CSE potential. CSEs were either heated or cooled, then measured against a room temperature CSE in a similar manner to Ewing. Pawel's result was the same as Ewing's, with a slope of " ~ 0.9 mV/°C" over a temperature range of 3–46 °C. Pawel's measurement of the copper sulfate concentration effect on CSEs yielded almost the same result as Ansuini and Diamond, 17 mV/(decade of g/L). Pawel also studied the effect of chloride contamination on the CSE potential and found that cells with significant excess copper sulfate were more resistant to a chloride contaminant than those with only a few crystals of excess copper sulfate. The oversaturated CSEs were relatively insensitive to chloride contamination, requiring concentrations of 1.0–2.0% chloride to produce a deviation of 15 mV in the CSE potential. Reported CSE potentials were found to be relatively insensitive to contaminations of up to 1.88% sulfide, 1.0% iron, sufficient sulfuric or nitric acid to bring the solution to pH ~ 1 , or sufficient sodium hydroxide to bring the solution to pH ~ 13 . Replacement of half the water in the electrolyte solution with antifreeze resulted in a 15 mV decrease in potential after a few days. These tests showed that the CSE potential was nearly unchanged after contamination with a variety of species, assuming sufficient excess of copper sulfate,

and can be used to measure the reference potential in a range of aqueous solutions. Pawel found that formation of different types of oxide films on the solid copper in the CSE had an effect of <5 mV on the CSE potential. The deviation was eliminated once the oxide films were scrubbed off the copper. Pawel also investigated the effect of light on the CSE potential and reported that overhead fluorescent or incandescent light had no measurable influence, while direct sunlight had a variable effect and which is attributable to heating rather than photoactivity.

The results of past studies of the CSE potential and their conditions are summarized in Table 1. The range of values reported below clearly suggests that additional measurements under well controlled conditions would be useful.

2. Materials and methods

In the current study, the electrical potential of the CSE relative to the SCE was measured as a function of temperature in 10 °C increments over the range of 5–45 °C. Three electrodes of each type were employed in order to minimize the experimental error. The copper sulfate electrodes (bold type) were connected to the calomel electrodes (underlined) via a potassium chloride salt bridge to make the following electrical couple:



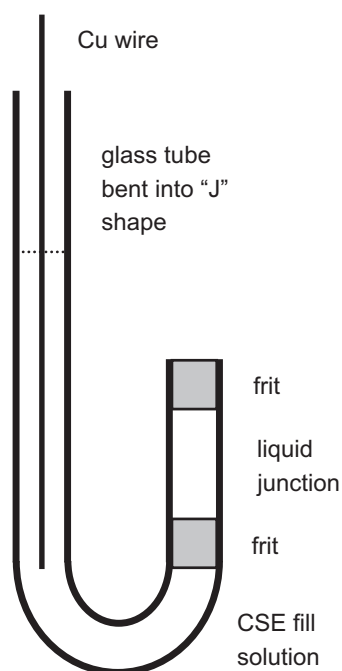
The single junction SCE electrodes (Radiometer Analytical, REF421) have an operating range of -10 °C to 60 °C. The saturated potassium chloride electrolyte solution was made by heating or cooling water to the temperature of interest and adding potassium chloride crystals to saturation. Since the bridge solution was the same as the SCE electrolyte solution, a double junction electrode was unnecessary.

The apparatus for determination of the potential difference between the CSE and the SCE was designed to measure a stable open circuit potential. To achieve this objective, it was important to maintain a constant temperature and to form reproducible liquid junctions. Liquid junctions are, by their nature, unstable and difficult to reproduce, since they are formed by the mixing of two liquids, in this case saturated copper sulfate and potassium chloride solutions. The liquid junction potential is dependent on the nature of the concentration transition layer between the solutions. Over a wide range of configurations reported, liquid junctions with cylindrical symmetry give the most reproducible results [9]. For this reason, a double liquid junction with frits on either end of a tube was used for the CSEs in this study instead of a single junction. A low porosity frit was chosen (Vycor[®] 7930 glass frits, average pore diameter of 40 Å) in order to minimize the concentration change of the CSE electrolyte filling solution during the experiments due to diffusion. The tube between the frits was filled with the CSE electrolyte solution at the start of the experiment.

The CSEs were specially fabricated for these experiments. The general design, shown in Fig. 1, consists of a 0.64 mm diameter copper wire (99.999%, oxygen free) in a 5 mm inner diameter glass tube bent into a "J" shape. A Vycor[®] glass frit (3.2 mm diameter by 6.4 mm long) was attached to the short end of the "J" with plastic tubing. A second frit was placed in series with the first one, a short piece of plastic tubing connecting the two; thus, the frits formed two liquid junctions. The length of the frits was sealed in heat-shrink Teflon[®] tubing. Copper sulfate crystals at the bottom of the "J" shaped glass tubing ensured saturation conditions and did not block the frits. To make the electrical connection with the potentiostat, a gold-plated screw BNC fitting was attached to the end of the copper wire. Further details of the CSE can be found in Stern [10].

Table 1
Reported CSE potentials.

Refs.	CSE versus SCE (mV)	Slope (mV/°C)	Conditions studied
[1]	75	0.9	1–51 °C
[3]	68–73	–	Ambient temperature
[4]	60 (theoretical)	0.97	4–49 °C (for the slope)
[7]	–	–	Effect of light, [CuSO ₄], [Cl ⁻]
[8]	–	~0.9	3–46 °C; effect of light, [CuSO ₄], [Cl ⁻], [S], [Fe], [acid/base], antifreeze, oxide film on Cu

**Fig. 1.** Schematic diagram of the copper sulfate double junction electrode.

The CSE electrolyte solution was made by adding crystals of copper sulfate pentahydrate to an aqueous solution of 69.5 mM sulfuric acid (at room temperature); the sulfuric acid solution was first brought to the experimental temperature and then the crystals were added until saturation was achieved. The presence of sulfuric acid prevented copper oxide formation on the copper wire. The density of the solution at each temperature was measured gravimetrically using a glass volumetric flask that was heated or cooled to the temperature of the solution prior to measurement. Copper concentration was measured using the bathocuproine method [11], which gives the mass percent of copper, or titration with ethylenediaminetetraacetic acid (EDTA), which gives the molarity of copper. The molarity of copper was converted to mass percent copper by using the measured density of the solution. The solubility of copper sulfate and the sulfuric acid concentration at each temperature was determined by combining the measured mass percent copper of the final solution, the ratio of copper sulfate to water as added via the copper sulfate pentahydrate crystals, and the sulfuric acid concentration of the solution before the addition of the crystals yielded the solubility of copper sulfate and the sulfuric acid concentration at each temperature. These concentrations were used as inputs for the electrolyte property modeling described in Section 3.

To ensure thermal and compositional equilibrium of the electrodes, the CSEs were placed in a stirred 1 L flask of saturated copper sulfate solution and the SCEs were placed in a stirred 2 L reaction kettle of saturated potassium chloride at temperature for at least 24 h prior to the beginning of the experiment. The flask and reaction kettle were both immersed in a 16 L agitated water

bath to regulate and maintain constant temperature. The bath temperature was regulated with a chiller and a glass stick heater.

The saturated potassium chloride solution was sparged with re-search grade argon gas for at least 45 min to remove dissolved oxygen prior to the transfer of the CSEs to the reaction kettle. The CSEs were removed from the saturated copper sulfate bath and rinsed thoroughly with 18.2 MΩ cm water. A thin layer of water was allowed to remain on the top of the frits since it was found that drying the ends of the frits introduced variability in the data. Once the CSEs were transferred to the reaction kettle, the argon sparge was replaced with an argon blanket. The blanket was kept in place for the duration of the experiment. The agitation in the reaction kettle was stopped during the measurement phase of the experiments to prevent convection currents from interfering with the electrical potential measurements. The temperature of the reaction kettle was maintained within 0.2 °C of the target at 5 °C and 25 °C and within 0.1 °C of the target at 15 °C, 35 °C, and 45 °C during the experiments. Temperature uniformity of the reaction kettle was improved by insulating the portion of the kettle that was above the water surface in the bath. For this study, laboratory light was assumed not to affect the potential of the CSE.

Three sets of data were measured – the open circuit potential difference between each of the CSEs and a single SCE, the difference between all of the SCEs, and the temperature of the saturated potassium chloride bridge solution. Each set of data was recorded for at least twenty-four hours to ensure a stable potential difference measurement at a stable temperature. The potentials were measured with a high-impedance potentiostat (model #197 Auto-ranging Microvolt DMM, Keithley; accuracy 0.02% of reading).

At the end of each experiment, the CSEs were removed and disassembled. The glass and plastic portions were rinsed with water and dried. The frits and copper wire were soaked in fresh, room temperature copper sulfate solution. The SCEs were removed from the reaction kettle, emptied, and filled with room temperature saturated potassium chloride solution. Their tips were left to soak in the same solution.

3. Theory

We could not experimentally measure the true equilibrium electrical potential between the CSE and SCE, since the mixing of the two different filling solutions is a non-equilibrium process, which gives rise to the liquid junction potential (LJP, E_j). The measured potential ($E_{measured}$) is composed of the equilibrium potential of the CSE relative to the NHE (E_{CSE}), minus the SCE potential, also relative to the NHE (E_{SCE}), plus E_j as shown in Eq. (2).

$$E_{measured} = (E_{CSE} - E_{SCE}) + E_j \quad (2)$$

Once E_j was determined, E_{CSE} could be estimated from Eq. (2). Two methods were used to calculate E_j . Method 1 was used to estimate the LJP, while Method 2 was used in an attempt to more precisely calculate the LJP. In Method 1, E_{CSE} was calculated, and then E_j was calculated using Eq. (2). This method used the Nernst equation, Eq. (1), to determine E_{CSE} , so it required the value of $a_{Cu^{2+}}$ in the CSE

filling solution over the range of experimental temperatures. The activity was calculated from electrolyte physical property modeling and E_{CSE}° assumed to be 0.340 V [6]. The Meissner Corresponding States electrolyte model was used as a first approximation of the a_i [12]. More detailed calculations were performed with Aspen-Plus™ 2004 using the Electrolyte Non-Random Two Liquid equation of state (ELECRTL) [13]. ELECRTL was chosen over the Pitzer electrolyte model because it is better able to simulate the behavior of concentrated solutions [14]. The ELECRTL results were then compared to the results of the Meissner model.

In Method 2, the LJP was calculated directly by integrating the right-hand side of Eq. (3) across the liquid junction solution as a function of the activity of all the solutes [6]. This method required the concentration, activity, and electrical mobility of each component of the KCl and CSE filling solutions as a function of distance between the electrolytes. It does not require E_{CSE}° as opposed to Method 1.

$$E_j = \frac{-RT}{F} \int_I^{\text{II}} \sum_{i=1}^y \frac{t_i}{z_i} d(\ln a_i) \quad (3)$$

$$t_i = \frac{|z_i|u_i c_i}{\sum_{i=1}^y |z_i|u_i c_i} \quad (4)$$

where I = copper sulfate electrode solution, II = saturated potassium chloride solution, t_i = transference number of species i , z_i = charge on species i , a_i = activity of species i , u_i = electrical mobility of ion i ($\text{cm}^2 \text{s}^{-1} \text{V}^{-1}$), c_i = concentration of species i ($\text{mol}(\text{kg water})^{-1}$), R = gas constant ($\text{J mol}^{-1} \text{K}^{-1}$), T = temperature (K), F = Faraday constant (C mol^{-1}), and y = total number of species.

The liquid junction in the experiments was formed by a vertical tube with a low porosity frit on either end. The saturated copper sulfate solution was in a reservoir at the bottom of the tube and the saturated potassium chloride solution was in a reservoir at the top of the tube. In order to integrate Eq. (3), several assumptions were made about the mass transport profile in the liquid junction. At each experimental temperature, the density of the saturated copper sulfate solution was greater than that of the saturated potassium chloride solution. The tube itself was stationary, as well, so it was assumed that there was no mass transport in the tube due to convection. The mixing of the two solutions, therefore, was driven solely by diffusion due to the concentration gradient. Furthermore, the mixing occurred over at least 24 h, so it was assumed that all chemical reactions were at equilibrium and that a stable chemical gradient was developed across the junction. In order to integrate Eq. (3), it was assumed that the concentration of all species varied linearly across the junction. This assumption means that the concentration of each species can be related to its position in the tube (x) through Eq. (5). By convention, $x = 0$ is the solution I interface (bottom of the tube above the lower frit) and $x = 1$ is the solution II interface (top of the tube below the upper frit).

$$c_i = c_i^I + (c_i^{\text{II}} - c_i^I)x \quad (5)$$

In addition, the electrical mobility of each species was assumed to be constant for all experimental concentrations and can be approximated by the mobility at infinite dilution. The ionic mobilities for many concentrated species are usually about 5–20% less than at infinite dilution [15]. The transport assumptions made in this derivation are the same as those made to derive the most commonly used simplified version of the liquid junction potential: the Henderson equation [16]. The derivation in this work differs from the Henderson derivation in that the activity of a component is not assumed to be equal to its concentration. The validity of the assumptions of linear concentration variation and constant electrical mobility of all species is evaluated in Section 4.2.

Combining Eqs. (3)–(5) yields Eq. (6), which is used to calculate the liquid junction potential for Method 2.

$$E_j = \frac{-RT}{F} \int_0^1 \sum_{i=1}^y \frac{\frac{|z_i|u_i c_i}{z_i} \left(\frac{d(\ln a_i)}{dx} \right)}{\sum_{i=1}^y |z_i|u_i c_i^I + x \sum_{i=1}^y |z_i|u_i (c_i^{\text{II}} - c_i^I)} dx \quad (6)$$

The electrical mobilities listed in Table 2 are for infinite dilution [6] except for that of Cu^{2+} , which was calculated based on the transference number for a CuSO_4 solution at 0.5 M using the infinite dilution mobility of SO_4^{2-} [15]. The electrical mobility of HSO_4^- is approximated as half that of SO_4^{2-} since the former is almost the same size but has half the charge. The electrical mobilities for the other charged species are known from literature.

Method 2 (Eq. (6)) requires c_i and a_i of all charged species as a function of x . For the saturated potassium chloride solution, c_i and a_i of potassium and chloride are known [17]. c_i and a_i of all of the charged species in the copper sulfate solution and the liquid junction solution were not available in the literature and were calculated with AspenPlus™ 2004 using ELECRTL [13], as with Method 1. The Meissner Corresponding States model was not used for Method 2 because data for all of the species were not available.

4. Results and discussion

4.1. Experimental

The measured density of the saturated copper sulfate solutions as a function of temperature is shown in Table 3.

The copper sulfate saturation concentration results from both the bathocuproine method (5–25 °C) and the EDTA method (35–45 °C) are shown as the mass percent of copper sulfate in Fig. 2. The measured values are slightly lower than those reported by Miles and Menzies [18], who measured saturated copper sulfate solutions with no sulfuric acid. The decreased copper sulfate solubility is expected, due to the common ion effect. Crockford and Warrick [19] measured copper sulfate solubility over ranges of temperature and sulfuric acid concentration that span those of the current study. Since Crockford and Warrick did not explore the same sulfuric acid concentration as this study, the copper sulfate solubility was interpolated at each temperature. There appears to be significant unexplained variation in their results, underscoring the need for our investigation.

Fig. 3 reports the values of the molalities of copper sulfate and sulfuric acid in the CSE electrolyte filling solution as a function of temperature. These were calculated from the measured mass per-

Table 2
Species mobilities.

Species	u ($\text{cm}^2 \text{s}^{-1} \text{V}^{-1}$)
K^+	7.619×10^{-4}
Cl^-	7.91×10^{-4}
Cu^{2+}	8.04×10^{-4}
SO_4^{2-}	1.654×10^{-3}
H_3O^+	3.625×10^{-3}
HSO_4^-	8.270×10^{-4}

Table 3
Saturated copper sulfate density.

Temperature (°C), ± 0.1	Solution density (g/mL), ± 0.005
5.0	1.16
10.0	1.17
15.0	1.19
25.0	1.21
35.0	1.25
45.0	1.28

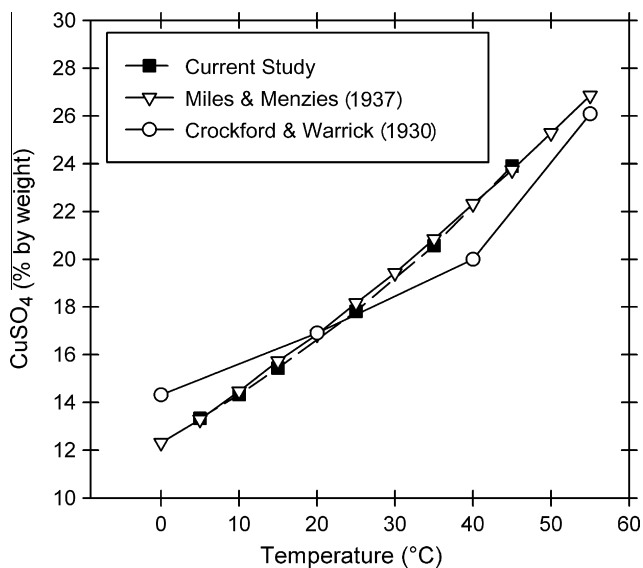


Fig. 2. Temperature dependence of the solubility of copper sulfate in water.

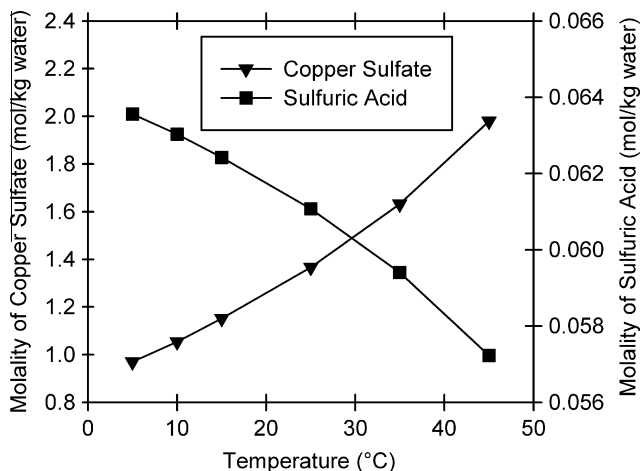


Fig. 3. Temperature dependence of the molality of copper sulfate and sulfuric acid at saturation condition.

cent of copper sulfate, the measured solution density, and the sulfuric acid concentration of the solution before the addition of copper sulfate.

The potential measurements for the CSE relative to the SCE are presented as a function of temperature in Figs. 4 and 5. The figures also include regression equations for the potential with standard deviations for the fit coefficients. Fig. 4 shows the linear regression fit, while Fig. 5 shows the second-order regression fit. Each point on each graph represents one CSE relative to the average of all three SCEs.

The electrical potential variation amongst the CSEs at a given temperature has an average standard deviation of 0.6 mV across all temperatures. This value is larger than the average absolute value of the potential difference amongst the SCEs, which is 0.2 mV. The accuracy of the electrical potential measurement was 0.02% of the value, or approximately 0.02 mV at the highest value.

The linear fit to the potential of the CSE versus the SCE is statistically significant, but the second order fit more accurately represents the theoretical behavior. Since the change in copper sulfate solubility is not linear with temperature (Fig. 3), it is to be expected

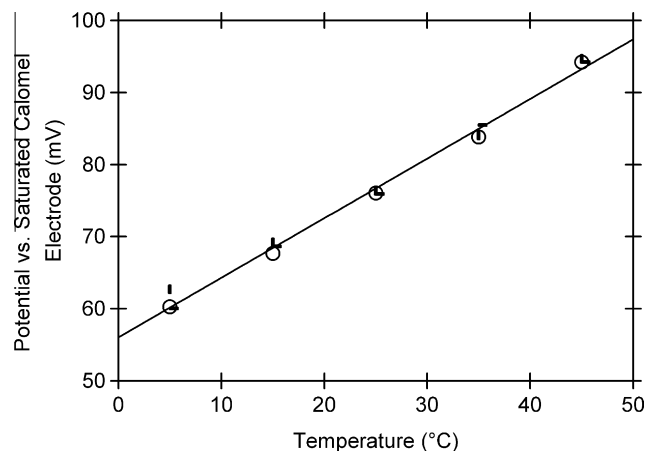


Fig. 4. Temperature dependence of the potential of the copper sulfate electrode versus the saturated calomel electrode by linear regression; $E_{CSE} = (0.83 \pm 0.02)T + (56.0 \pm 0.5)$; $R_{adj}^2 = 0.993$.

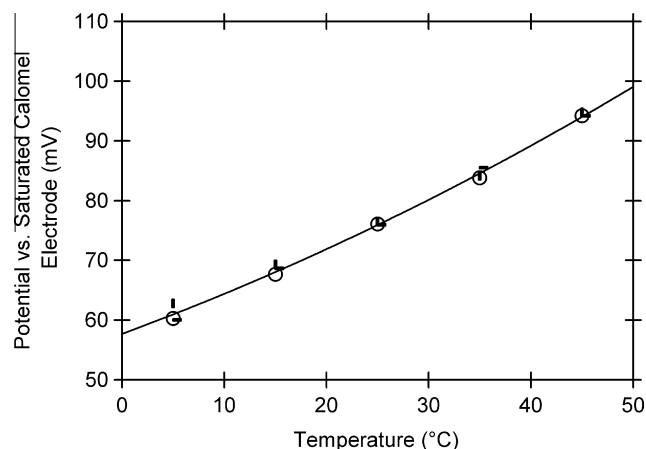


Fig. 5. Temperature dependence of the potential of the copper sulfate electrode versus the saturated calomel electrode by second order regression; $E_{CSE} = (0.004 \pm 0.001)T^2 + (0.63 \pm 0.06)T + (57.7 \pm 0.6)$; $R_{adj}^2 = 0.996$.

that the potential is nonlinear. The slope of the linear fit is 0.83 ± 0.02 mV/°C, consistent with the value of 0.9 mV/°C found by Ewing [1] and Pawel [8].

Previous work has related the SCE to the NHE, with no LJP effects, over the range of 5–70 °C [17]. Within an error of 0.1 mV, the two electrodes are related by

$$E_{SCE} \text{ (mV)} = 241.2 - 0.661(T - 25) - 1.75 \times 10^{-3}(T - 25)^2 - 9.0 \times 10^{-7}(T - 25)^3 \quad (7)$$

where T is in degrees Celsius. Eq. (7) was used to convert the data from this study from the SCE reference to the NHE reference. The linear fit of the potential of the CSE versus the NHE (in mV and degrees Celsius) with the standard deviation excluding the error introduced by Eq. (7) is

$$E_{CSE} = (0.17 \pm 0.01)T + (313.4 \pm 0.4) \quad (8)$$

and the second order fit is

$$E_{CSE} = (0.002 \pm 0.001)T^2 + (0.06 \pm 0.06)T + (314.3 \pm 0.6) \quad (9)$$

The data shown in Figs. 4 and 5 were converted to the NHE reference using Eq. (7). Those average values are shown in Table 4. The error at each temperature is the standard deviation of the experimental measurements plus the error of Eq. (7).

Table 4
Average measured potential.

Temperature (°C)	Potential (CSE versus NHE, mV)
5.0	314.5 ± 1.3
15.0	315.9 ± 0.7
25.0	317.1 ± 0.2
35.0	318.7 ± 1.2
45.0	321.5 ± 0.2

The measured potential of the CSE versus NHE of 317 mV at 25 °C is bracketed by Ewing's value of 316 mV and the other commonly accepted value of 318 mV [20,21]. The potential of the CSE versus the NHE has less variation with temperature than that of either the SCE or the silver–silver chloride electrode. The relatively small temperature dependence of the CSE is beneficial because it means that precise temperature control is not required for accurate potential measurements using the CSE.

4.2. Theoretical

The LJP for the CSE was calculated using inputs from both the ELECRTL and the Meissner equations of state, as described in Section 3. The database in AspenPlus™ 2004 was used for all the inputs into ELECRTL except for the two equilibrium constants representing potassium chloride and copper sulfate solubility. Use of the default value for the equilibrium constant for potassium chloride solubility (K_{KCl}) resulted in a potassium chloride solubility limit much lower than the standard literature value [22]. A regression was performed on data for the mean activities of potassium and chloride ions, assuming unit activity for potassium chloride [17]. The resulting equation for K_{KCl} was substituted for the standard AspenPlus™ 2004 values in all calculations, as shown in Eq. (10). In AspenPlus™ 2004, the KCl equilibrium reaction is written as a dissociation reaction, so the equilibrium constant equation is given by

$$\begin{aligned} \ln K_{KCl} &= \ln \left(\frac{a_{K^+} a_{Cl^-}}{a_{KCl}} \right) = \ln (a_{K^+}^2 a_{Cl^-}) \\ &= -34.3 - \frac{0.679}{T} + 6.38 \ln T \end{aligned} \quad (10)$$

The AspenPlus™ 2004 database assumed complete dissociation for copper sulfate in solution. However, spectrophotometric studies by Dadgar et al. and by Méndez De Leo et al., have shown that copper sulfate can be present as a neutral ion pair species in solution [23,24]. Méndez De Leo assumed the activity coefficient of the neutral ion pair copper sulfate in solution (γ_{CuSO_4}) was equal to one in order to calculate the equilibrium constant (K_{CuSO_4}). The limited K_{CuSO_4} data available at atmospheric pressure were used to develop an expression for K_{CuSO_4} as a function of temperature, as in Eq. (11). Eq. (11) was used to model the neutral copper sulfate dissociation in AspenPlus™ 2004.

$$\begin{aligned} \ln K_{CuSO_4} &= \ln \left(\frac{a_{CuSO_4}}{a_{Cu^{2+}} a_{SO_4^{2-}}} \right) = \ln \left(\frac{c_{CuSO_4} \gamma_{CuSO_4}}{c_{Cu^{2+}} \gamma_{Cu^{2+}} c_{SO_4^{2-}} \gamma_{SO_4^{2-}}} \right) \\ &= -20.9 + \frac{0.381}{T} + 4.61 \ln T \end{aligned} \quad (11)$$

The equilibrium constant for copper sulfate pentahydrate ($CuSO_4 \cdot 5H_2O(s)$) solubility was left at its default value and yielded results slightly above the experimental values.

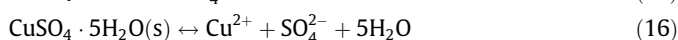
The activities of all components in solution were computed under four different sets of conditions, or Cases, as described in Table 5. The conditions were varied such that half employed an equilibrium constraint for neutral copper sulfate in solution and half did not. Within each subset, one condition used the value of copper

Table 5
Model conditions for ELECRTL model.

Case #	CuSO ₄ equilibrium included?	CuSO ₄ concentration
1	Yes	Simulated saturation
2	Yes	Set to match experimental value
3	No	Simulated saturation
4	No	Set to match experimental value

sulfate concentration based on the simulation, and the other used the value of copper sulfate concentration determined experimentally. Every condition was evaluated at 10 °C increments from 5 to 45 °C.

The set of reactions (Eqs. (12)–(16)) was used to calculate the activities of the saturated copper sulfate and sulfuric acid system over the range of temperatures from 5 °C to 45 °C, assuming the presence of neutral copper sulfate species in solution (Cases 1 and 2). All species are in aqueous solution unless marked with (s) to indicate a solid.



For Cases 3 and 4, in which there is no neutral copper sulfate present, Eq. (15) was assumed to be an irreversible dissociation. The other reactions were unchanged.

Fig. 6 shows the values of the activity of Cu^{2+} calculated for each case using the ELECRTL model. Cases 1 and 3 give similar results to each other, as do Cases 2 and 4. The total concentration of copper is the dominant factor for the calculation of $a_{Cu^{2+}}$ using the ELECRTL model. The speciation of copper plays a minor role in the calculations.

The Meissner model [12] was used as well to calculate the mean activity coefficient of copper sulfate ($\gamma_{Cu^{2+}SO_4^{2-}}$) in a sulfuric acid solution. $a_{Cu^{2+}}$ was then determined from $\gamma_{Cu^{2+}SO_4^{2-}}$ using a Debye–Hückel framework as shown in Eq. (17), where γ_i is the activity coefficient of species i .

$$\gamma_{Cu^{2+}} = e^{-\left(\frac{z_{Cu^{2+}}^2}{z_{Cu^{2+}SO_4^{2-}}}\right) \ln(\gamma_{Cu^{2+}SO_4^{2-}})} = \gamma_{Cu^{2+}SO_4^{2-}} \quad (17)$$

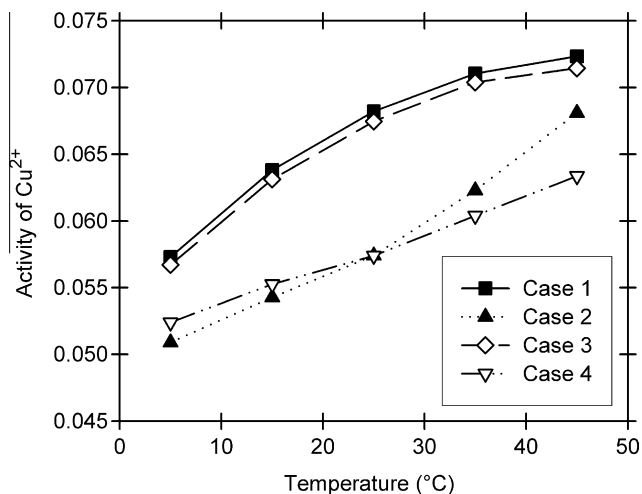


Fig. 6. Temperature dependence of the activity of Cu^{2+} as calculated by the ELECRTL model.

The reaction system used for the Meissner model (Eqs. (18) and (19)) is simplified from that used in the ELECNRTL model (Eqs. (12)–(16)).



HSO_4^- was not used in the Meissner model because no data for $\text{Cu}(\text{HSO}_4)_2$ are available. Copper sulfate was modeled using available data [12]. Extended Debye–Hückel behavior was assumed for sulfuric acid because its concentration was moderately low (molality ~ 0.6) and the ionic strength of sulfuric acid does not follow the Meissner model [25]. The experimental values for the copper sulfate and sulfuric acid concentrations over a range of temperatures (Fig. 3) were used as inputs to the Meissner model.

Fig. 7 shows the results of the calculations of $a_{\text{Cu}^{2+}}$ using the Meissner and ELECNRTL models with Method 1. The experimental values of $a_{\text{Cu}^{2+}}$ in Fig. 7 were calculated by applying the Nernst equation (Eq. (1)) to the measured potentials. Both the Meissner and ELECNRTL models predict an $a_{\text{Cu}^{2+}}$ that is significantly less than the experimental values. The Meissner model predicts a slightly negative temperature dependence, whereas the ELECNRTL model is more consistent with experimental results with a slightly positive temperature dependence. In part, the difference between the values calculated from the experiment and those from the models can be attributed to the LJP, which is not accounted for in the Nernst equation. The models consider only the steady-state thermodynamic contribution to the electrical potential and ignore the transient transport contribution.

Eq. (1) can be used to convert the calculated values of $a_{\text{Cu}^{2+}}$ to E_{CSE} . Each calculation set is then summarized as a function of temperature, and the correlation constants are shown in Table 6.

As with $a_{\text{Cu}^{2+}}$, the models underpredict the value of E_{CSE} at all temperatures. The ELECNRTL model and the Meissner model both show a negative temperature dependence for E_{CSE} , unlike $a_{\text{Cu}^{2+}}$, where only the Meissner model showed a negative dependence. The experimental data (Table 4) showed a positive temperature dependence. The models are able to predict the enthalpic contribution (ΔH) to the potential within 10% but poorly predict the entropic (ΔS) contribution because they do not match the temperature dependence as illustrated in Eq. (20).

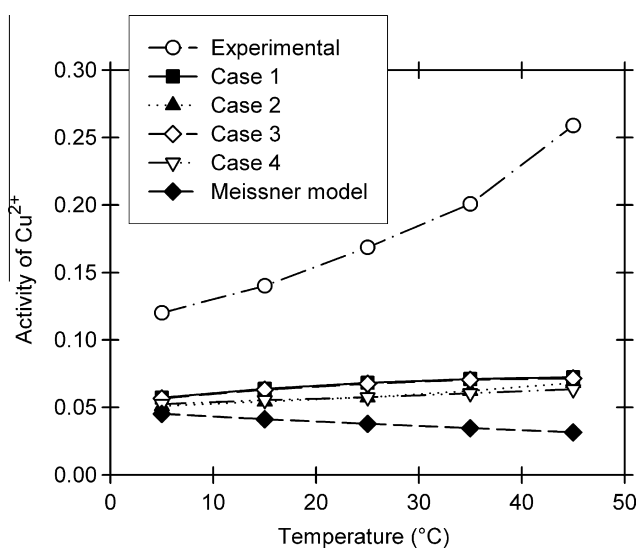


Fig. 7. Temperature dependence of the activity of Cu^{2+} : a comparison of experimental data, values calculated by the ELECNRTL model, and values calculated by the Meissner model.

Table 6
Comparison of the trendline parameters for E_{CSE} .

Condition	Slope (mV/°C)	Intercept (mV) versus NHE	Average difference from experiment (mV)
Experiment	0.17	313	–
Case 1	–0.04	306	–13
Case 2	–0.03	304	–14
Case 3	–0.05	306	–13
Case 4	–0.06	305	–14
Meissner model	–0.26	304	–20

$$E = -\frac{\Delta H}{nF} + \frac{T\Delta S}{nF} \quad (20)$$

The best match of prediction to the experimental results is from Case 1, although, as with activity, there is little difference between its results and those from Case 3. The ELECNRTL model with the AspenPlus™ 2004 database, overall, does a decent job of modeling $a_{\text{Cu}^{2+}}$ (within 94% for all temperatures), though there is still room for improvement, including modeling the proper temperature dependence. Since the model does not include the LJP, it is expected that the model predictions will differ from the experimental results.

All the cases analyzed produced similar values of E_{CSE} . Even though the inclusion of the neutral copper sulfate in solution does not have a significant effect on the calculated CSE potential, it will have a significant impact on the LJP because it changes the ratio of neutral (CuSO_4) to charged (Cu^{2+} , SO_4^{2-}) species. As described above, using Method 1, the LJP can be estimated using the differences between the experimental and calculated values for E_{CSE} (Table 6). Since the LJP is concentration dependent, Case 2, which is based on the experimental value of copper in solution and included the neutral solvated CuSO_4 equilibrium, was chosen as the model to calculate the LJP. Case 2 is the most similar to actual conditions, and it differs from the experimental result by -14 mV, on average, over the temperature range of this study. Therefore, -14 mV is taken as an estimate of the LJP.

Method 2, a direct calculation of the LJP, was used in an attempt to further refine the estimate of LJP obtained by using Method 1. To calculate the LJP directly, all parameters and functions in Eq. (6) must be either measured or calculated. The (calculated/measured) electrical mobility used for each species is listed in Table 2. The concentrations of the charged species in the SCE electrolyte solution are known from experimental measurements. The concentrations of the charged species in the CSE electrolyte solution were determined from a combination of experimental measurements and calculations with ELECNRTL (using the conditions for Case 2). The concentration of each species as a function of position x was calculated using Eq. (5) at increments of 0.1 in x with the points 0.01, 0.95, and 0.99 added. The natural logarithms of the activities of all species were fit using a fifth order polynomial. The integral in Eq. (6) was calculated using Maple software (Waterloo Maple Inc. 2000). Since the smallest deviation between the experimental and calculated values of E_{CSE} was at 5 °C, it is likely that more accurate results can be obtained at that temperature than at the higher temperatures. The liquid junction potential was found to be equal to 9 V at 5 °C. This value is several orders of magnitude larger than the experimental results indicate is possible, so each model assumption was examined to determine its validity.

The liquid junction potential calculated using Model 2 is highly sensitive to the mobility of the ions. For instance, changing the copper ion mobility from its value at 0.5 M ($8.0 \times 10^{-4} \text{ cm}^2 \text{ s}^{-1} \text{ V}^{-1}$) to its value at infinite dilution ($9.9 \times 10^{-4} \text{ cm}^2 \text{ s}^{-1} \text{ V}^{-1}$) shifts the liquid junction potential to 13 V. The sensitivity of the model to the ionic mobility suggests that the mobility must be measured, not approximated, as was done with the infinite dilution values

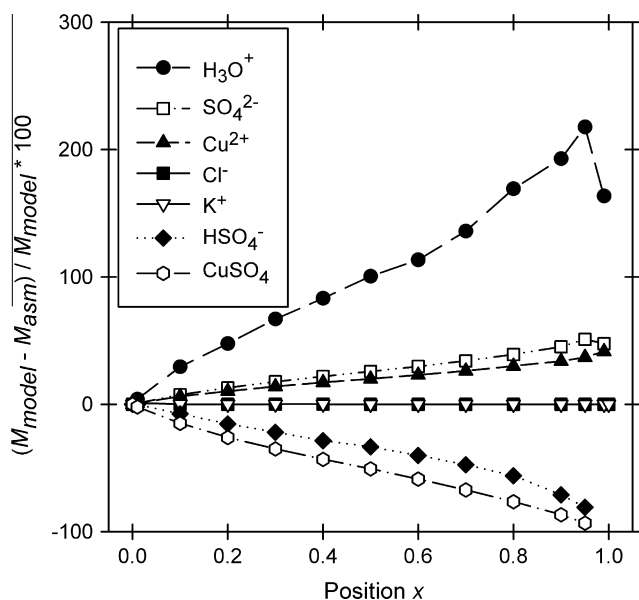


Fig. 8. Percent deviation of model molality (M_{model}) from assumed molality (M_{asm}) as a function of position x .

for most species. Measuring the ionic mobilities was beyond the scope of this work.

Another significant source of error in Method 2 arises from the assumption of linear variation of the concentration of all species across the liquid junction (Eq. (5)). While this assumption is valid for the potassium chloride species, it ignores the equilibrium reactions of the neutral copper sulfate species and sulfuric acid. At each position x the inputs to the ELECNRTL model are the total concentration of solid copper sulfate and of pure sulfuric acid. The model then determines the equilibrium concentration and activity of each species in solution. Fig. 8 shows a plot of the percent deviation of the concentration in molality predicted by the ELECNRTL model (M_{model}) from the linearly estimated concentration (M_{asm}) as a function of x . Deviations of over 200% are observed. These deviations probably lead to large errors in the calculated liquid junction potential. Since Eq. (5) is not valid for copper sulfate and sulfuric acid, Eq. (6) (Method 2) is not valid.

A better way to approach the calculation of the LJP for this system is digital simulation of the behavior of the liquid junction region (see Britz [26]). The general approach for digital simulation is to divide x into small sections and simultaneously solve for the concentration and activity of all species in each section. The simulation would include the ELECNRTL model for the reaction system, the diffusion equation for transport of the species between each section, and the boundary conditions of the composition of the electrolyte solutions at either end of the liquid junction region. Digital simulation was beyond the scope of this work.

5. Conclusions

The potential of the CSE was measured as a function of temperature from 5 °C to 45 °C versus the SCE. The values of the potential of the CSE versus the NHE were calculated. Data were fit with both first- and second-order models. The linear regressed slope of 0.17 ± 0.01 mV/°C in reference to the NHE was found to be similar to previously measured values that used slightly different experimental setups [1,8]. The value found for the potential of the CSE

in reference to the NHE at 25 °C, 317.1 ± 0.2 mV, is bracketed by the commonly accepted values of 316 and 318 mV [2,20,21]. It is recommended that this value of the CSE be used for all future studies that employ the CSE as a reference electrode in an aqueous solution.

Two methods were employed to estimate the LJP of the CSE at the potassium chloride solution interface. Method 1 provided an estimate of the LJP of -14 mV. Method 2, which was used in the hope of finding a more accurate result than Method 1, failed to yield a reasonable value because the assumption of linear concentration variation of all species across the LJP was shown to be invalid. Further work using digital simulation would be required to obtain a more refined estimate of the LJP and, thus, the thermodynamic value of the CSE potential.

Method 1 could be applied to the development of any new reference electrode that forms a salt bridge with a stable potential versus a known reference electrode. As shown in this paper, Method 2 requires that the concentration of the species in the salt bridge must vary linearly from one end of the salt bridge to the other. Method 1 requires that the activities for the electroactive species can be calculated or well estimated, whereas Method 2 also requires thermodynamic and ionic transport data for all species in the salt bridge.

Acknowledgments

The authors wish to acknowledge the contributions of Michael Mock and the Martin Family Foundation for fellowship support to one of the authors (H.A.G.S.).

References

- [1] S. Ewing, Am. Gas Assoc., Proc. 21 (1939) 624.
- [2] H.H. Uhlig, R.W. Revie, Corrosion and Corrosion Control An Introduction to Corrosion Science and Engineering, John Wiley & Sons, New York, 1985.
- [3] L.P. Aker, Corrosion 13 (1957). Tech. Topics.
- [4] G.N. Scott, Corrosion 14 (1958) 136t.
- [5] W.M. Latimer, The Oxidation States of the Elements and Their Potentials in Aqueous Solutions, Prentice-Hall, New York, 1952.
- [6] A.J. Bard, L.R. Faulkner, Electrochemical Methods: Fundamentals and Applications, John Wiley & Sons, Inc., New York, 2001.
- [7] F.J. Ansuini, J.R. Dimond, Mater. Perform. 33 (1994) 14.
- [8] S.J. Pawel, R.J. Lopez, E. Ondak, Mater. Perform. 37 (1998) 24.
- [9] E.A. Guggenheim, J. Am. Chem. Soc. 52 (1930) 1315.
- [10] H.A.G. Stern, Chemical Engineering, Massachusetts Institute of Technology, Cambridge, 2006.
- [11] A.E. Greenberg, L.S. Clesceri, A.D. Eaton, M.A.H. Franson (Eds.), Standard Methods for the Examination of Water and Wastewater, American Public Health Association, Washington, DC, 1992.
- [12] J.W. Tester, M. Modell, Thermodynamics and its Applications, Prentice Hall, Upper Saddle River, New Jersey, 1997.
- [13] Aspen Technology, Aspen Technology, Cambridge, MA, 2004.
- [14] V. Abovsky, Y. Liu, S. Watanasiri, Fluid Phase Equilib. 150–151 (1998) 277.
- [15] E.W. Washburn (Ed.), International Critical Tables of Numerical Data, Physics, Chemistry and Technology, vol. 6, McGraw-Hill, New York, 1929.
- [16] D.A. MacInnes, The Principles of Electrochemistry, Dover, New York, 1961.
- [17] H. Chateau, J. Chim. Phys. Phys.-Chim. Biol. 51 (1954) 590.
- [18] F.T. Miles, A.W.C. Menzies, J. Am. Chem. Soc. 59 (1937) 2392.
- [19] H.D. Crockford, L.E. Warrick, J. Phys. Chem. 34 (1930) 1064.
- [20] E.C. Potter, Electrochemistry Principles and Applications, Cleaver-Hume Press Ltd., London, 1956.
- [21] D.A. Jones, Principles and Prevention of Corrosion, Prentice Hall, Upper Saddle River, NJ, 1996.
- [22] W.F. Linke, Solubilities Inorganic and Metal-Organic Compounds, American Chemical Society, Washington, DC, 1965.
- [23] A. Dadgar, D. Khorsandi, G. Atkinson, J. Phys. Chem. 86 (1982) 3829.
- [24] L.P. Méndez De Leo, H.L. Bianchi, R. Fernández-Prini, J. Chem. Thermodyn. 37 (2005) 499.
- [25] H.P. Meissner, J.W. Tester, Ind. Eng. Chem. Process Des. Develop. 11 (1972) 128.
- [26] D. Britz, Digital Simulation in Electrochemistry, Springer-Verlag, Berlin, Heidelberg, 2005.